



Resurfacing receptor binding domain of Colicin N to enhance its cytotoxic effect on human lung cancer cells



Wanatchaporn Arunmanee^a, Methawee Duangkaew^a, Pornchanok Taweecheep^a, Kanokpol Aphicho^a, Panuwat Lerdvorasap^a, Jesada Pitchayakorn^a, Chayada Intasuk^a, Runglada Jiraratmetacon^a, Armini Syamsidi^b, Pithi Chanvorachote^{c,d}, Chatchai Chaotham^{a,d}, Natapol Pornputtapong^{a,e,*}

^a Department of Biochemistry and Microbiology, Faculty of Pharmaceutical Sciences, Chulalongkorn University, Bangkok 10330, Thailand

^b Department of Pharmacy, Faculty of Science, Tadulako University, Central Sulawesi 94118, Indonesia

^c Department of Pharmacology and Physiology, Faculty of Pharmaceutical Sciences, Chulalongkorn University, Bangkok 10330, Thailand

^d Cell-based Drug and Health Products Development Research Unit, Faculty of Pharmaceutical Sciences, Chulalongkorn University, Bangkok 10330, Thailand

^e Center of Excellence in Systems Biology, Faculty of Medicine, Chulalongkorn University, Bangkok 10330, Thailand

ARTICLE INFO

Article history:

Received 7 May 2021

Received in revised form 5 September 2021

Accepted 8 September 2021

Available online 14 September 2021

Keywords:

Pore forming toxin

Colicin

Protein resurfacing

Anticancer

ABSTRACT

Colicin N (ColN) is a bacteriocin secreted by *Escherichia coli* (*E. coli*) to kill other Gram-negative bacteria by forcefully generating ion channels in the inner membrane. In addition to its bactericidal activity, ColN have been reported to selectively induce apoptosis in human lung cancer cells via the suppression of integrin modulated survival pathway. However, ColN showed mild toxicity against human lung cancer cells which could be improved for further applications. The protein resurfacing strategy was chosen to engineer ColN by extensive mutagenesis at solvent-exposed residues on ColN. The highly accessible Asp and Glu on wildtype ColN (ColN^{WT}) were replaced by Lys to create polycationic ColN (ColN⁺¹²). Previous studies have shown that increase of positive charges on proteins leads to the enhancement of mammalian cell penetration as well as increased interaction with negatively charged surface of cancer cells. Those solvent-exposed residues of ColN were identified by Rosetta and AvNAPSA (Average number of Neighboring Atoms Per Sidechain Atom) approaches. The findings revealed that the structural features and stability of ColN⁺¹² determined by circular dichroism were similar to ColN^{WT}. Furthermore, the toxicity of ColN⁺¹² was cancer selective. Human lung cancer cells, H460 and H23, were sensitive to ColN but human dermal papilla cells were not. ColN⁺¹² also showed more potent toxicity than ColN^{WT} in cancer cells. This confirmed that polycationic resurfacing method has enabled us to improve the anticancer activity of ColN towards human lung cancer cells.

© 2021 The Author(s). Published by Elsevier B.V. on behalf of Research Network of Computational and Structural Biotechnology. This is an open access article under the CC BY-NC-ND license (<http://creativecommons.org/licenses/by-nc-nd/4.0/>).

1. Introduction

Over the last decade, therapeutic protein products especially monoclonal antibodies (mAb) have revolutionized cancer therapy by minimizing harmful side effects, enhancing target specificity, and increasing potency [1]. In 2020, the therapeutic landscape has been gradually shifting to antibody-based therapeutics with 12 new approved mAb for cancer and infectious disease while only 2 new products received approval in the period between 2006 and 2010 [2]. Despite these advantages, these proteins with complex structure and post-translational modification often required expensive and sophisticated mammalian cell production and

purification processes [3,4]. Due to their relatively large size (approximately 150 kDa), their penetration and localization into solid tumor is limited, resulting in poor tumor response to antibody therapy [5,6]. An alternative strategy to overcome these drawbacks is the development of novel protein therapeutics. Pore-forming toxins are one such novel protein candidates that show promising potential in cancer therapy. Pore forming toxins produced by sea anemones, bacteria, spider and human cells has been reported to exhibit *in vitro* cytotoxic effect towards leukemia [7], breast cancer [8,9], lung cancer [10–12], and colon cancer cells [13]. With the advent of recombinant technology, these toxins can be easily fused with fragment antibodies and targeting molecules used for targeted cancer therapy. These hybrid toxins could be produced in more cost-effective and highly scalable microbial expression sys-

* Corresponding author.

E-mail address: natapol.p@chula.ac.th (N. Pornputtapong).

tems which would be more affordable and accessible in developing countries.

Colicins are toxins produced and secreted by *Escherichia coli* to kill other Gram-negative bacteria. Apart from their antibacterial activities, pore-forming colicins e.g. colicin A, E1 and N has shown cytotoxic effects on several cancer cells such as breast, bone, colon and gastric cancers [14–18]. Lancaster *et al.* and Arunmanee *et al.* also reported that the cytotoxicity of colicins was more specific towards cancer cells than normal cells [17,19]. Colicin N (ColN), being the smallest colicin, has the advantage of high tumor penetration and being able to reduce immunogenicity [20]. However, the mild cytotoxic effect of ColN on cancer cells currently limits their clinical use. To improve its cytotoxic effect on cancer cells, protein engineering can be exploited to tailor and enhance desired properties of ColN.

Protein resurfacing was chosen to enhance the selectivity and cytotoxicity of ColN towards human lung cancer cells. This protein engineering strategy has been used to modify protein properties such as stability, solubility, selective recognition, and penetration of mammalian cells [21]. Protein resurfacing can be done by mutagenesis of solvent-exposed residues located on the protein surface [22]. Incorporation of polycationic features on proteins has been considered to facilitate mammalian cell penetration [23]. For example, the substitution of solvent exposed amino acids with arginine in green fluorescence proteins can enhance cellular uptake [24]. Onconase, an anticancer amphibian RNase with polycationic-decorated surface showed more efficient cell-uptake potency compared to the wild-type protein [25,26]. Furthermore, increase in positive charges of the protein surface also promotes its cancer-selective toxicity [27]. This is caused by the initial electrostatic interaction between polycationic proteins and negatively charged cancer cell membrane [28]. The exposure of negatively charged phospholipids, mainly phosphatidylserine (PS), on the outer leaflet of the plasma membrane can only be found in cancer cells and not in normal cells [29]. Therefore, the polycationic feature of proteins could alter the selectivity and toxicity of proteins against cancer cells.

In this study we have replaced the solvent-exposed aspartic and glutamic acids of ColN with lysine at the receptor binding domain. This increased the net positive charge on the surface of ColN with an aim to target and enhance the cytotoxic effect on human lung cancer cells. Those solvent-exposed residues of ColN can be identified by computational Rosetta and AvNAPSA (Average number of Neighboring Atoms Per Side-chain Atom) approaches [23,30]. Polycationic resurfaced ColN (ColN⁺¹²) were then engineered and produced in *E. coli*. The secondary structure and stability of ColN⁺¹² in comparison with wild-type ColN (ColN^{WT}) were investigated. Furthermore, the selectivity and cytotoxicity of ColN⁺¹² and ColN^{WT} were also assessed on human lung cancer cells and normal cells.

2. Materials and methods

2.1. Computational redesign of charge mutated colicin N

The structure-guided protein design was performed based on the previously published crystal structure of colicin N (PDB 1A87) [31]. The Supercharge application [22] under Rosetta software suite [30] were used to identify non-stabilizing, exposed, negatively charged residues in the receptor binding domain of ColN. The running options of Rosetta Supercharge were set to default. The Supercharge determined the optimum positions for the charge incorporation using AvNAPSA approach which selected the highly exposed polar residues whilst minimizing structural changes [23,30]. The appropriate solvent-exposed residues for sub-

stitution were ranked by AvNAPSA values. The aspartate residues with high AvNAPSA values were replaced by lysine residues. During the replacement, the supercharge calculated the updated reference energy and the correct net charge by pack rotamers mover. The potential residues that proposed by Rosetta Supercharge were used in homology modeling to create the mutant structure for further molecular dynamic analysis.

2.2. Homology modelling and in silico structure analysis

The homology model of the sextuple mutant ColN was constructed via SWISS-MODEL [32]. The model was built with ProMod3 using 1A87 [31] as a template. Qualitative Model Energy Analysis (QMEAN) scoring function [33] was used to assess global and per-residue model quality. Further structure analysis and visualization was performed using PyMol [34,35]. Root Mean Square Deviation were calculated to assess structural similarity between predicted model and wild-type crystal structure. Electrostatic surface potential maps were built with solvent-excluded surface and Adaptive Poisson–Boltzmann Solver using APBS electrostatics PyMol plug-in [36,37].

2.3. Cloning

DNA fragments of ColN gene (222 – 531 bps) with mutations of D154K, E115K, D150K, E96K, D159K, and D102K were synthesized by Twist Biosciences, USA. This construct was subcloned into pET3a by using the Gibson Assembly Master Mix kit (New England BioLabs, Ipswich, MA). Two set of primers including 1) 5'-CGAGG TAATAACGGTGATGGAGCGAGTGCTAAGGTTG-3' and 5'-CAAGTT TATTGTTATATTTCCGTCCTCCAGTTCAC-3', and 2) 5'-GTGAACGT GAAGGGACCG-3' and 5'-CCTTAGCACTCGCTCCATCACC GTTAT TACCTCGATTTC-3', were used to amplify gene fragments and plasmids by PCR, respectively. Following manufacturing protocols, the two PCR products were mixed with Gibson Assembly Master Mix to generate plasmids encoding ColN with desired mutations.

2.4. Expression and purification of colicin N

Plasmids encoding ColN gene with a c-terminal his-tags were transformed into BL21-AITM One Shot[®] chemically competent *E. coli* (Invitrogen, USA). The transformed cells were grown at 37 °C overnight. The overnight culture was further grown in LB media containing 100 µg/mL ampicillin at 37 °C until OD₆₀₀ = 0.6–0.8. To induce protein expression, arabinose was added to the bacterial culture to the final concentration of 0.2% (w/v) arabinose. After induction for 3 h, cells were harvested by centrifugation at 8,000 g for 10 min and resuspended in 50 mM sodium phosphate buffer, pH 8.0, 300 mM NaCl, 10 mM imidazole supplemented with DNase I, RNase, and PierceTM Protease Inhibitor Tablets (Thermo Scientific, MA, USA). The pellets were sonicated for 15 min and the lysate was collected after centrifugation at 17,000 g for 20 min at 4 °C. To purify the protein by Fast Protein Liquid Chromatography (FPLC), the lysate was then injected onto a nickel-sepharose HisTrapTM FF affinity column (GE Healthcare Technologist, West Milwaukie, WI, USA) previously equilibrated with 50 mM sodium phosphate buffer, pH 8.0, 300 mM NaCl, 10 mM imidazole. The column was washed by 50 mM sodium phosphate buffer, pH 8.0, 300 mM NaCl, 25 mM imidazole. The protein was then eluted with the same buffer consisting of 250 mM imidazole. The protein containing fractions were collected and then dialyzed against Phosphate Buffer Saline (PBS; 10 mM Na₂HPO₄, 2 mM KH₂PO₄, 137 mM NaCl, 2.7 mM KCl, pH 7.4) at 4°C overnight. The purity and amount of protein were assessed by SDS-PAGE and bicinchoninic acid (BCA) protein assay kit (Thermo Scientific, MA, USA), respectively.

2.5. Circular dichroism

Each protein sample at 0.5 mg/mL was prepared in PBS. All measurements were performed on a CD spectrophotometer (j-815CD Spectrophotometer, Jasco, Tokyo, Japan), using the quartz cuvettes with a pathlength of 0.1 cm. Spectra were collected at a range of temperature from 20 to 90 °C in 10 °C increment over the wavelength range of 260 to 190 nm. The temperature stability at 220 nm was monitored at 10-degree intervals (from 20 °C to 90 °C; 8 measurements) and temperature ramp was set to 1 °C per min.

2.6. Limited proteolysis of wild-type colicin N and polycationic colicin N

60 µg of purified proteins in PBS were digested by 0.02 µg trypsin in the same buffer at room temperature. At 0, 30, 60, 90, 120, 150 and 180 min after mixing with trypsin, 20 µL of samples were collected. To stop the digestion at each time point, 20 µL of gel loading buffer were immediately added to samples and then the mixture was heated at 95 °C for 10 min. All samples were loaded on 12% SDS-PAGE and stained with Coomassie Brilliant Blue G-250 to visualize the bands of proteins.

2.7. Agar overlay assay

Antimicrobial test of recombinant ColN were performed using agar overlay techniques which was previously described in Hockett, K. L. and Baltrus, D. A., 2017 [38]. Briefly, a single colony of *E. coli* NCTC 10538 was grown in 5 mL of LB media overnight at 37 °C. The overnight culture was then diluted at 1/100 into fresh LB and incubated for 3–4 h. 100 µL of bacterial culture was inoculated into the 3 mL of soft agar (0.7% (w/v) agar in ultrapure water). The resulting mixture was poured onto solidified LB agar plates. Once overlay agar solidified, 2 µL of recombinant ColN in phosphate buffered saline pH 7.4 were spotted onto the overlay. The plates were incubated overnight at 37 °C prior to observe clear zones.

2.8. Cell culture and treatment

Human lung cancer H460 and H23 cells were obtained from American Type Culture Collection (Manassas, VA, USA) while human dermal papilla cells (hDPCs) were obtained from Applied Biological Materials Inc. (Richmond, Canada). Roswell Park Memorial Institute (RPMI) 1640 medium (Gibco, Gaithersburg, MA, USA) was used to maintain H460 and H23 cells whereas DPCs cell was cultured in Prigrow III medium (Applied Biological Materials Inc., Richmond, BC, Canada). All culture mediums were supplemented with 10% fetal bovine serum (FBS), 2 mmol/L of L-glutamine and 100 units/mL of penicillin/streptomycin (Gibco, Gaithersburg, MA, USA). The cells were maintained in an incubator at 37 °C under humidified atmosphere of 5% CO₂ until reaching 70–80% confluence for use in experiments.

Cytotoxic effect of prepared colicin N in lung cancer and dermal papilla cells was examined by crystal violet colorimetric assay which is presented as a quick and reliable method for screening the effect of compound on cell survival and growth inhibition [39]. Firstly, cells were seeded at a density of 1×10^4 cells/well in 96-well plate and then treated with ColN^{WT} and ColN⁺¹² mutant for 24 h. After washing with sterile deionized water for 2 times to remove detachable dead cells, the remain living cells were fixed with 1% formaldehyde for 30 min. The cells were then stained with 0.05% (w/v) crystal violet (Sigma-Aldrich Corp., St. Louis, MO, USA). After 10 min incubation at room temperature, the cells were washed with sterile deionized water twice and air dried overnight.

Crystal violet staining biomass was solubilized and shake with 200 µL of methanol at room temperature for 15 min. The absorbance of was measured via spectrophotometry at 570 nm using a microplate reader (Anthros, Durham, NC, USA). The percentage (%) of cell viability was calculated from the absorbance ratio between treated and untreated control cells.

Mode of cell death was detected via nuclear co-staining of Hoechst33342 and propidium iodide (Sigma-Aldrich Corp., St. Louis, MO, USA). Briefly, cells were placed at a density of 1×10^4 cells/well in the 96-well plate for 12 h. Then, the cells were treated with ColN^{WT} and ColN⁺¹² mutant at concentration 0–10 µM. After 24 h incubation, the treated cells were then incubated with Hoechst33342 (10 µg/mL)/ propidium iodide (5 µg/mL) solution at 37 °C for 30 min. The condensed chromatin and/or fragmented DNA at late stage of apoptosis exhibited bright blue fluorescence of Hoechst33342 while red fluorescence of propidium iodide-positive cells presented necrosis cells under fluorescence microscope (Olympus IX51 with DP70, Olympus, Japan) examination.

2.9. Statistical analysis

The data from three independent experiments are presented as means ± standard deviation (SD). Using SPSS statistical software version 22 (IBM Corp., Armonk, NY, USA), One-way analysis of variance and least significant difference (LSD) post hoc test were performed, with statistical significance at $p < 0.05$.

3. Results

3.1. Polycationic resurfacing of colicin N

To increase the net charge of ColN while remaining its folding and functions, Rosetta approach were utilized to identify the most exposed residues on its surface. In this approach, the first step is to define the surface of protein using AvNAPSA surface definition. The residues with low AvNAPSA scores indicate that these residues are further away from neighboring residues hence these residues are highly accessible to solvents and feasibly amendable to substitution. The selected residues were then assessed for the possibility of forming sidechain-sidechain and sidechain-backbone hydrogen bonds which play a vital role in the protein structure and stability. The highly solvent-exposed residues, without the interaction with nearby residues via hydrogen bonds, were chosen for protein resurfacing. In this study, polycationic resurfacing was carried out at receptor binding domain (R) of ColN. The R domain of ColN is located in between translocation (T) and pore-forming (P) domains of ColN. The R domain was the target of mutagenesis since its high-resolution structure has been resolved and it was not involved in the main function of this protein [31]. On the other hand, T domain is intrinsically disordered whereas P domain is responsible for ColN toxicity. The amino acid sequence and crystal structure of ColN (PDB code: 1A87) were analysed. The solvent-exposed aspartic (D) and glutamic (E) acids of R domain were substituted by lysine residues (K) as these substitutions increased the net positive charge of the protein surface. According to the AvNAPSA scores computed by Rosetta (the cut-off was set at (120), there were seven D and E residues having AvNAPSA scores <120. These seven residues including E96, D102, E115, E126, D150, D154 and D159 were then predicted by Rosetta Supercharge whether they tend to form hydrogen bonds with either side chains or backbone of proteins. E96 and E115 showed the possibility of forming H-bonds. However, E96 is in the parts of intrinsically disordered ColN hence it is flexible and amendable to substitutions. Fig. 1a demonstrates the 6 points of mutations from D and E to K residues in this study. As D and E were changed to K, the charge

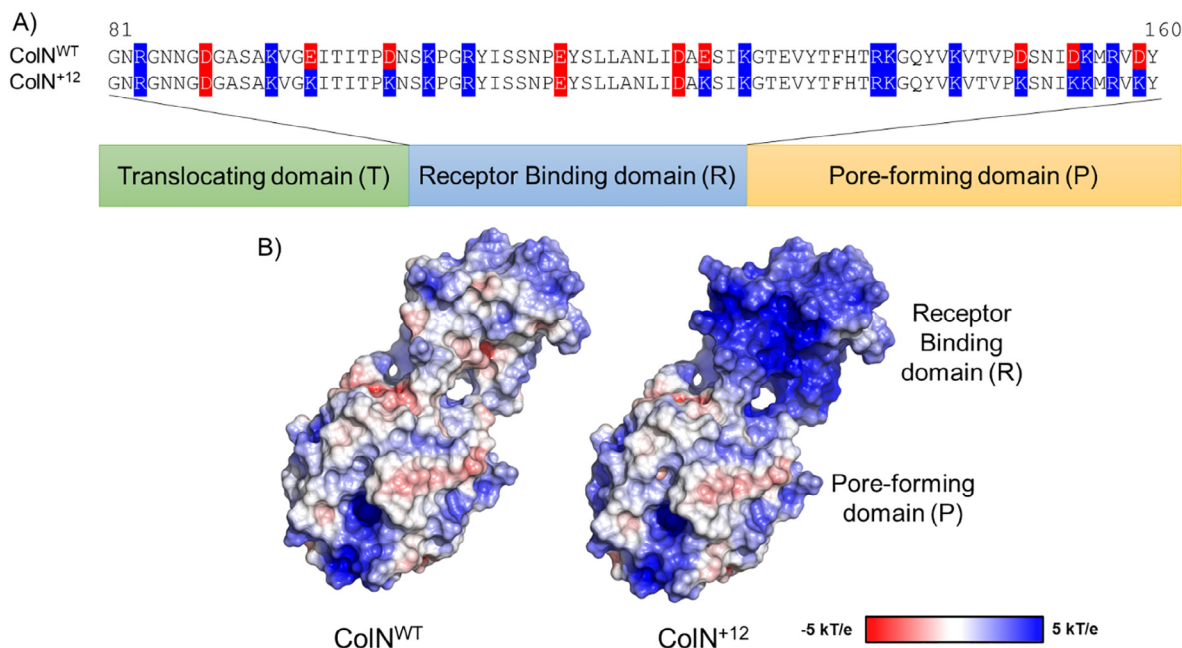


Fig. 1. Residues on the receptor-binding domain (R) of colicin N that were mutated to lysine to create the resurfaced polycationic colicin N (ColN⁺¹²). A) Amino acid sequence alignment of ColN^{WT} and ColN⁺¹² with mutation at D154K, E115K, D150K, E96K, D159K, and D102K. The R domain of ColN is located between translocating and pore-forming domains of ColN. Negatively and positively charged residues were highlighted in red and blue, respectively. B) The electrostatic surface potential maps of ColN^{WT} and ColN⁺¹² illustrate polycationic surface (blue) of ColN (PDB code: 1A87). (For interpretation of the references to colour in this figure legend, the reader is referred to the web version of this article.)

of R domain increase + 2 per substituting position. In total, net charge of polycationic ColN (ColN⁺¹²) are + 12 when compared to wild-type ColN (ColN^{WT}). A model of ColN⁺¹² was homology modeled by SWISS-MODEL to illustrate the mutated amino acids in tertiary structure. The QMEAN score pass the cutoff representing the model quality, both entirely and per-residue, and was deemed to pass the threshold for further analysis. A calculated RMSD of 0.140 Å suggests high similarity between the mutant model and wild-type crystal structure. The electrostatic surface potential maps as shown in Fig. 1b displayed the cationic charges on the surface of ColN comparing between ColN^{WT} and ColN⁺¹².

3.2. Polycationic resurfacing does not alter structure and stability of colicin N but does change proteolytic profiles

To examine the structural features of ColN^{WT} and ColN⁺¹², the pET3a plasmids encoding both ColN genes were constructed for protein production. According to the prediction from Rosetta approach, E96, D102, E126, D150, D154 and D159 were substituted by K resulting in ColN⁺¹² with E96K, D102K, E126K, D150K, D154K and D159K mutations. The mutations at six selected residues were carried out by Gibson Assembly. Gene fragment with the substitution of D and E codons with K codon were synthesized and then

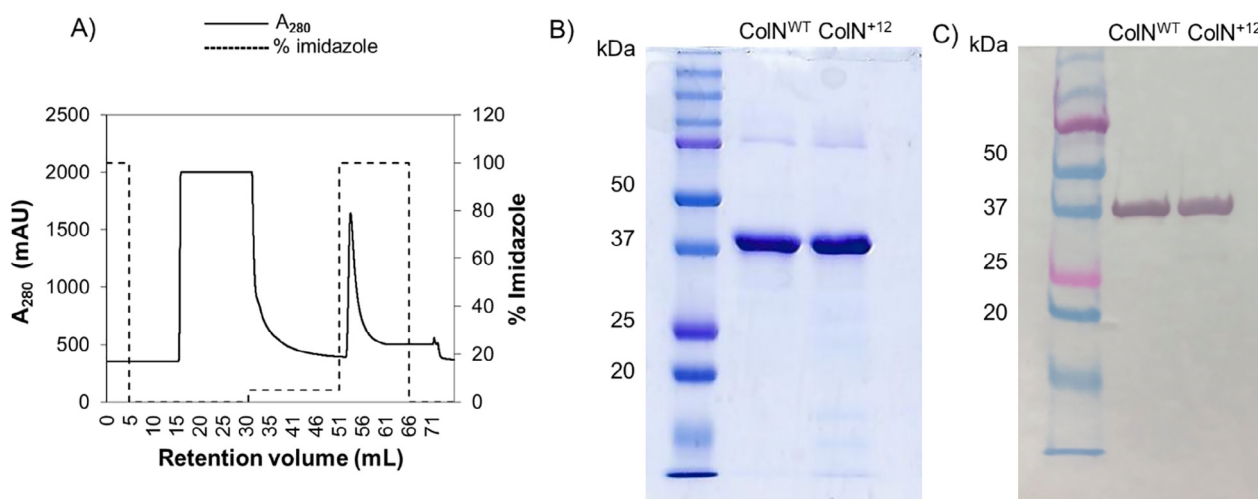


Fig. 2. Purification and identification of recombinant ColN with c-terminal histidine tag. A) Elution profiles of ColN using the 1-mL nickel-sepharose HisTrapTM FF affinity column equilibrated with 50 mM sodium phosphate buffer, pH 8.0 with 300 mM NaCl and 10 mM imidazole. Recombinant proteins were eluted when applying the same buffer containing 250 mM imidazole from 0% to 100%. B) SDS-PAGE analysis of protein-containing fractions obtained from affinity chromatography. C) Western blot analysis of ColN^{WT} and ColN⁺¹² detected by anti-6xHis antibody.

subcloned into plasmids encoding ColN gene. The DNA sequencing results of ColN⁺¹² showed accurate substitution sequences at desired positions. To examine the secondary structure and stabilization of ColN^{WT} and ColN⁺¹², both proteins were expressed in *E. coli* and purified. The pET3a plasmid encoding ColN^{WT} and ColN⁺¹² with c-terminal 6xhistag were expressed in *E. coli* BL21-AI. Proteins were then loaded on to a Ni column where proteins with 6xhistag were bound. The protein-containing fractions including flowthrough (FT) and elution fractions (EF) were collected. The identity and purity of recombinant proteins in each fraction were initially assessed by SDS-PAGE. Fig. 2A demonstrates

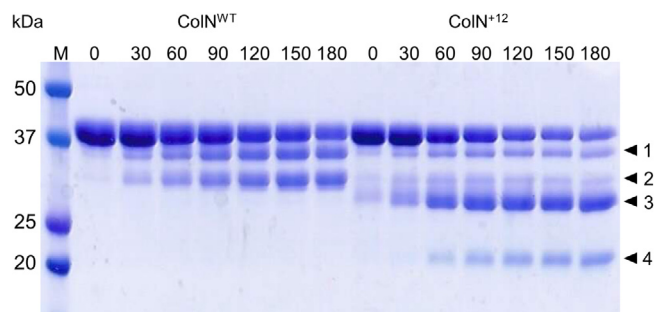


Fig. 3. Proteolysis of wild-type colicin N and its polycationic variant. 12% SDS-PAGE gel displaying the proteolysis fragments of colicin N by incubating with trypsin over 0–180 min. The main proteolytic fragments were located at black arrows no. 1–4.

the elution profile of ColN⁺¹² purified by FPLC. His-tagged proteins were retained in the column and eluted when increasing the concentration of imidazole in running buffer. The purified proteins in the eluted fraction analyzed by SDS-PAGE (Fig. 2B) were run at approximately 40 kDa corresponding to their theoretical mass of 42 kDa. To identify these proteins, analysis by western blot using anti-histag antibodies (Fig. 2C) indicated that each protein ran at their corresponding size and were bound by anti-histag antibodies. Moreover, the limited proteolysis of ColN^{WT} and ColN⁺¹² by trypsin were carried out to observe proteolytic profiles of proteins. As ColN⁺¹² possesses more accessible lysine than ColN^{WT}, ColN⁺¹² is likely to be digested at more sites by trypsin. Fig. 3 shows that the peptide mixtures from trypsin digested ColN^{WT} and ColN⁺¹² migrated on SDS-PAGE differently. These confirmed that proteins were successfully expressed and purified as a soluble protein in *E. coli*. According to the proteolytic profiles, the molecular weight of proteolytic fragments at position 1 and 2 were approximately equal to fragments cleaved at lysine residues within T domain of ColN. This domain is intrinsically disordered hence both fragments appeared in both ColN^{WT} and ColN⁺¹². In contrast, with the additional solvent-exposed lysines in ColN⁺¹², the additional bands, predominantly in the region of 20–30 kDa, appeared on the gel at the position 3 and 4. The smear bands were also observed between the band 2 and 3 in the ColN⁺¹² sample which could be generated from several cleavable locations at the mutated R domain of ColN⁺¹². The results clearly show that ColN⁺¹² seemed to be more sensitive to proteolysis than ColN^{WT}.

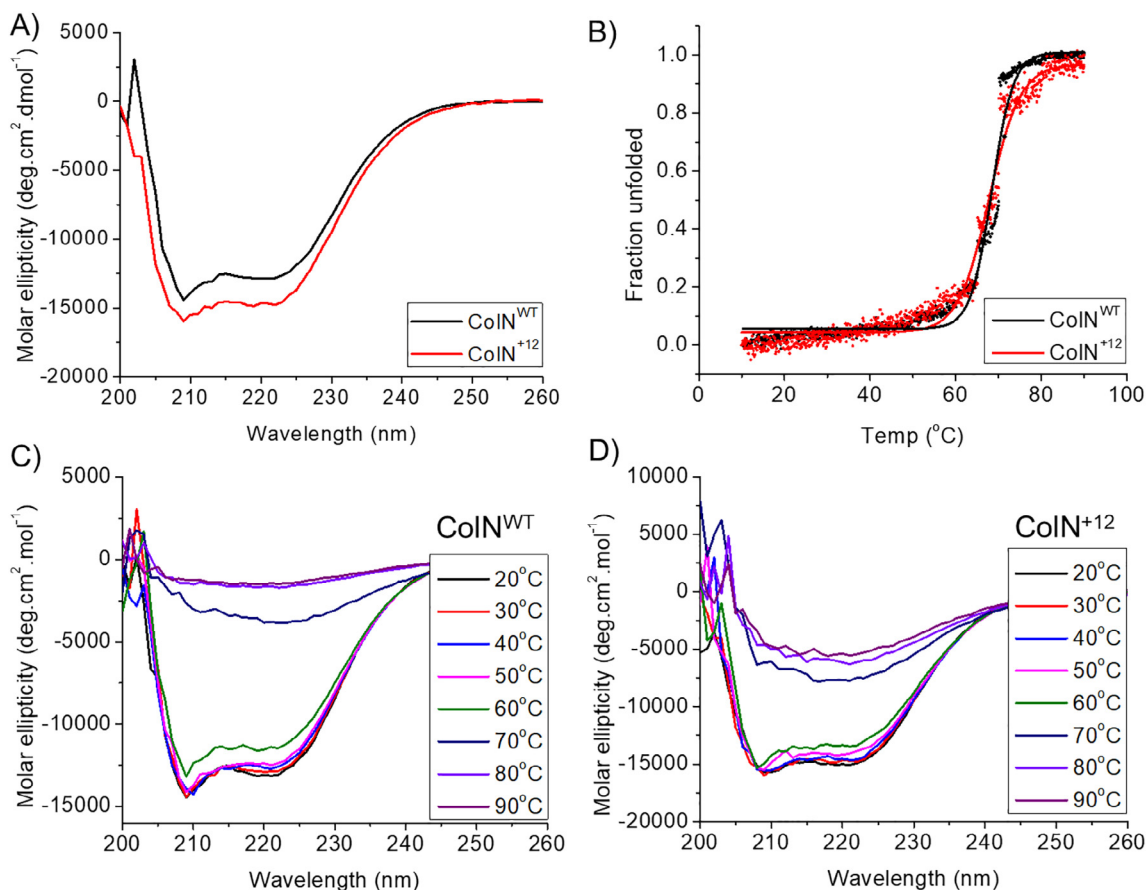


Fig. 4. Far-UV CD spectra of colicin N, measured in a 0.1 cm path-length cuvette at 25 °C over the wavelength range of 260 to 190 nm. The protein concentration was typically 0.5 mg/mL in PBS. Data are shown as A) the comparison between ColN^{WT} (black) and ColN⁺¹² (red); B) CD melting curves of ColN^{WT} (black) and ColN⁺¹² (red). Temperature scan performed from 10 to 90 °C at 220 nm in forward directions; and far-UV spectra of ColN^{WT} (C) and ColN⁺¹² (D) were recorded at different temperature. (For interpretation of the references to colour in this figure legend, the reader is referred to the web version of this article.)

Far-UV CD spectroscopy were performed to monitor the secondary structure content of ColN. Fig. 4A compares the far-UV CD spectra of ColN^{WT} and ColN⁺¹². The high-resolution structure of ColN from residue 90 to 387 (PDB code: 1A87) possess the beta sheet around a helix in receptor binding domain and 10 helical bundle in pore-forming domain whereas disordered translocating domain was not seen in the crystal structure [31]. Both ColN^{WT} and ColN⁺¹² exhibit a α spectrum showing minima at 222 and 208 nm due to the main structure of 10 helical bundle. However, far-UV spectra of ColN^{WT} and ColN⁺¹² were not identical implying that their secondary structure could be slightly different at the mutation sites in R domain. Regarding the thermal stability of both proteins, CD measurements at 220 nm were performed at varied temperatures from 10 to 90 °C. The plots between the molecular ellipticity and temperature can be used to determine the melting temperature of both proteins. Fig. 4B indicates that ColN^{WT} and ColN⁺¹² have the similar melting temperature at approximately 65 °C despite six substitutions in ColN⁺¹². In a good agreement with melting curve, the comparison of far-UV CD spectra at the range of temperature from 20 to 90 °C (Fig. 4C and D) also revealed that the transition from folded and unfolded state of both ColN^{WT} and ColN⁺¹² was in between 60 and 70 °C.

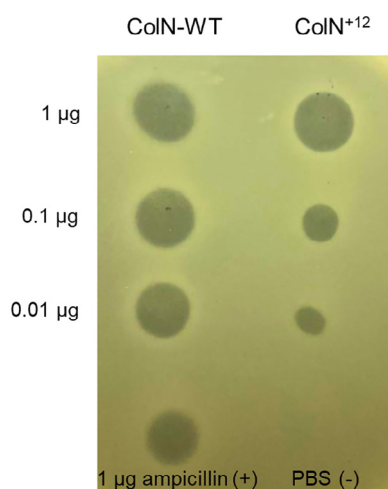


Fig. 5. The effect of mutations in colicin N on their bactericidal activity. Spot test assays of wild-type colicin N, ColN^{WT} (left) and colicin N mutant, ColN⁺¹² (right) illustrating the zone of inhibition on the lawn of *E. coli* NCTC 10538 strains after spotting 0.01, 0.1, and 1 µg of ColN in 50 mM sodium phosphate, pH 7.5, 300 mM NaCl.

3.3. Polycationic resurfacing reduces antimicrobial activity but enhance cytotoxic effect on cancer cells with cancer-selective properties

We next assessed the biological activities of recombinant ColN^{WT} and ColN⁺¹². To begin with the noted antibacterial activity of ColN, the agar overlay assay (Fig. 5) was carried out by spotting ColN solutions onto the lawn of *E. coli* NCTC 10538. *E. coli* were susceptible to both ColN^{WT} and ColN⁺¹² but ColN^{WT} was more potent than ColN⁺¹² when comparing their zones of inhibition on agar plates. The reduction of antimicrobial activity could be due to the structural change at receptor-binding domain of ColN⁺¹². In the case of cytotoxicity against human lung cancer cells, H460 (p53 and KRas wild-type) and H23 (p53 and KRas mutant) cells were maintained in culture medium containing 0–10 µM of ColN^{WT} and ColN⁺¹² for 24 h. Both ColN^{WT} and ColN⁺¹² reduced viability in H460 and H23 cells in dose-dependent manner (Fig. 6A and B). The decrease of %cell viability determined by crystal violet assay was significantly shown in lung cancer cells exposed with 10 µM ColN^{WT} and 5–10 µM ColN⁺¹². When comparing to at same concentrations, treatment with ColN⁺¹² exhibits more reduction of viable cells than ColN^{WT} treatment in both H460 and H23 lung cancer cells. Detection of mode of cell death demonstrated that culture either with ColN^{WT} (10 µM) or ColN⁺¹² (5–10 µM) obviously induced apoptosis presenting bright blue Hoechst33342 with barely detected red fluorescence of PI-positive necrosis in lung cancer H460 and H23 cells (Fig. 7D and E). Consistent with the viability results, %apoptosis was dramatically increased in H460 and H23 cells incubated with 5–10 µM ColN⁺¹² compared with ColN^{WT}-treated cells (Fig. 7A and B).

Inducing cell death in dermal papilla cells coincides with a common side effect of current chemotherapeutic drugs, namely hair loss, which can cause psychological distress in lung cancer patients [40–43], the safety profiles of ColN^{WT} and ColN⁺¹² were evaluated in human dermal papilla DPCs cells. The cultures were treated with 0–10 µM of ColN^{WT} and ColN⁺¹². Fig. 6C showed no significant alteration of %cell viability in DPCs cells cultured either with 1–10 µM of ColN^{WT} or ColN⁺¹². Additionally, neither ColN^{WT} nor ColN⁺¹² significantly augmented %apoptosis (Fig. 7C) or induced necrosis cell death in DPCs cells compared with non-treated control cells (Fig. 7F). The ratio of lung cancer cell apoptosis to dermal papilla cell apoptosis was calculated and presented as the values of cancer specificity for ColN^{WT} and ColN⁺¹². The value of cancer specificity for 5 µM ColN^{WT} are 10.24 and 11.86 in ColN^{WT}-treated lung cancer H460 and H23 cells, respectively. In comparison to ColN^{WT}, the treatment of ColN⁺¹² at 5 µM to H460 and H23 cells presents the greater value of cancer specificity at 64.51 and 61.67. These results suggest that ColN⁺¹² possesses more potent specific anticancer activity against human lung cancer cells.

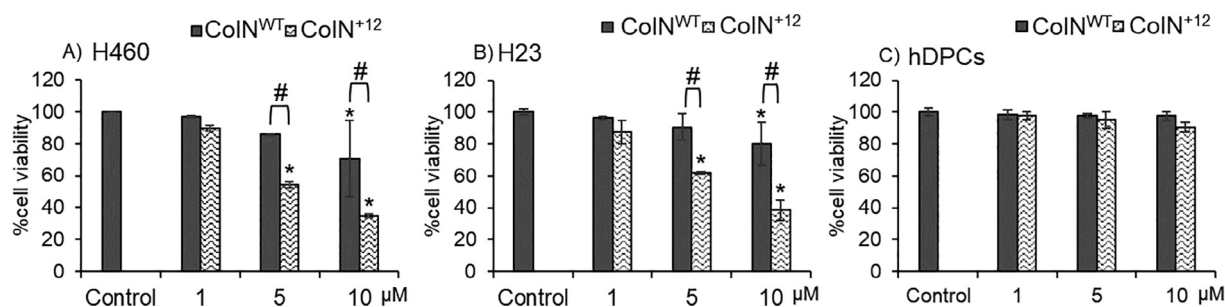


Fig. 6. Cytotoxicity profile of full-length Colicin N (ColN^{WT}) and Colicin N mutant (ColN⁺¹²) at concentration of 1–10 µM for 24 h against human lung cancer A) H460, B) H23, and C) human dermal papilla DPC cells. Values are means of the independent triplicate experiments \pm SD. * $p < 0.05$ versus non-treated control cells. # $p < 0.05$ versus ColN^{WT}-treated cells.

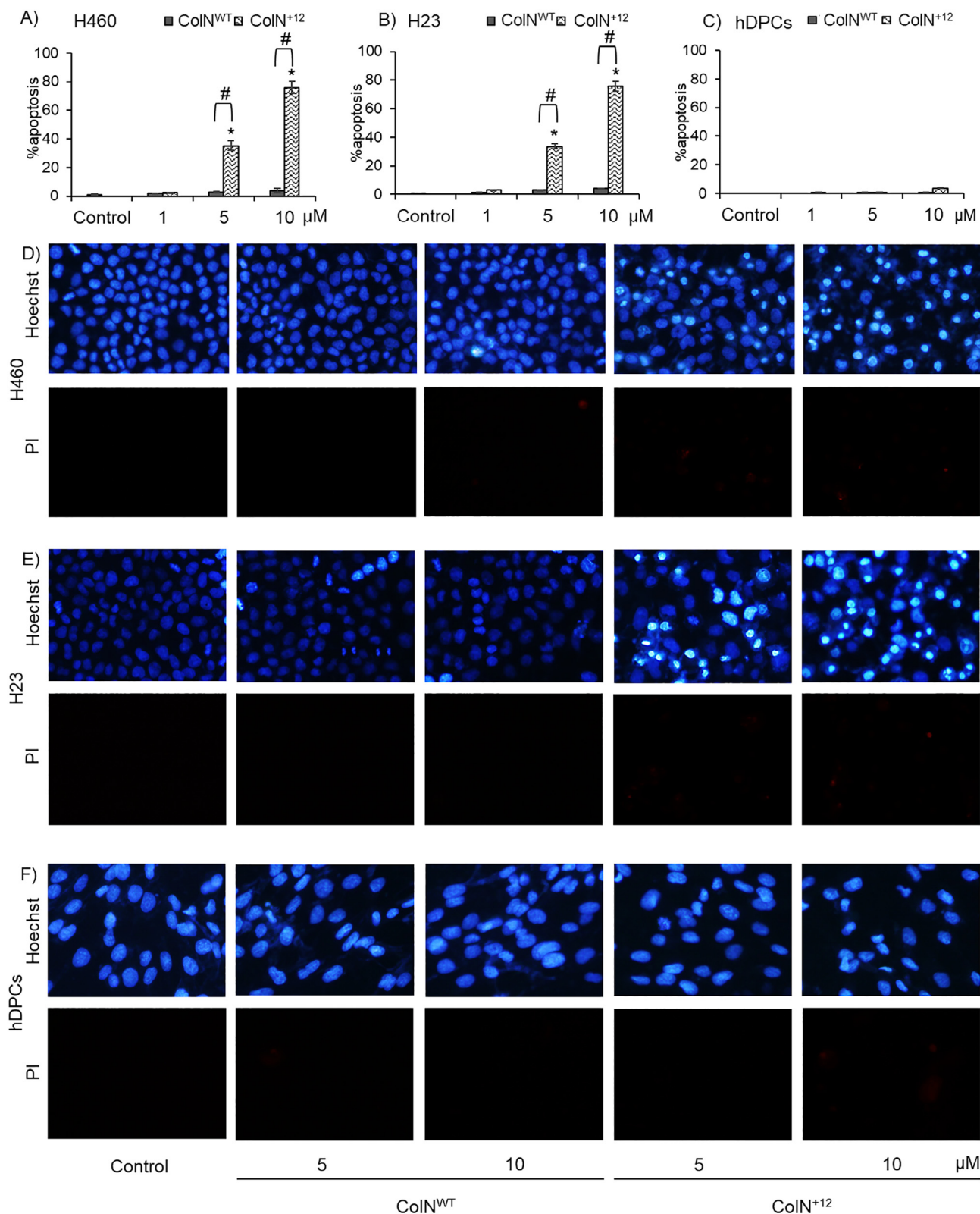


Fig. 7. Comparison of apoptosis-inducing effect between wild-type colicin N and its polycationic variant in human lung cancer cells. The %apoptosis cell presented after treatment with 5–10 μM CoIN⁺¹² mutant as concentration-dependent manner in A) H460, B) H23 and C) human dermal papilla DPCs cells compared with both untreated control and CoIN^{WT}-treated cells. The nuclear staining assay shows bright blue fluorescence of Hoechst33342 which represents condensed chromatin and/or fragmented nuclei containing in apoptosis D) H460 and E) H23 cells cultured with CoIN⁺¹² at 5–10 μM while there was no detectable necrosis stained with red fluorescence of propidium iodide (PI). The selective anticancer activity of CoIN^{WT} and CoIN⁺¹² was evidenced with C) no alteration of %apoptosis as well as F) non-observable apoptosis and necrosis cells stained with Hoechst/PI co-staining in DPCs cells. Values are means of the independent triplicate experiments ± SD. *p < 0.05 versus non-treated control cells. #p < 0.05 versus CoIN^{WT}-treated cells. (For interpretation of the references to colour in this figure legend, the reader is referred to the web version of this article.)

4. Discussions

Bacterial pore-forming toxins with anticancer activity has been proposed as alternative therapeutic agents since these toxins exhibit promising toxicity and selectivity towards cancer cells and they can be economically produced in *E. coli* [7,8,10,11,13]. Pore-forming toxin from *E. coli*, ColN, with mild cytotoxicity against cancer cells was chosen in this study. Here we modified the receptor binding domain of ColN by protein resurfacing methods with an aim to improve cytotoxicity and selectivity against human lung cancer cells.

Protein resurfacing is an emerging tool to engineer naturally occurring proteins with unusually high net charges. The resurfaced proteins exhibited an ability to withstand thermal denaturation, enable the penetration to mammalian cells, and improve their biological activities [21]. Due to the lack of established strategies for the extensive mutagenesis to create polycationic proteins, Asp and Glu in this study were designed for mutagenesis based on i) their AvNAPSA scores of <120, implying that they reside on the surface of ColN, ii) their unlikelihood of hydrogen bond formation with either neighboring sidechain and backbone, and iii) their location at receptor binding domain which are not involved in the pore formation of ColN. When candidate residues were selected according to the above criteria, the substitution between an arginine or lysine were considered. Several studies have shown that resurfaced proteins with arginine are preferable as arginine-rich proteins tend to be better in cell surface binding and cell penetration [25,44]. However, a relatively large side chain of arginine can potentially cause steric clashing to neighboring residues therefore lysine would be chosen for modification [45]. The mutation sites at R domain of ColN are close to each other, our simple resurfacing design were then achieved by replacing surface-exposed residues to lysine.

Although the advances in *in silico* design of polycationic proteins by mutagenesis are promising, little is known about how to maintain protein function and stability after considerably resurfacing a protein with high positive charges [45]. Therefore, the structural features and stability of ColN⁺¹² compared to ColN^{WT} needed to be determined. This study demonstrated that both wild-type and resurfaced proteins have a CD spectra similar to a previously reported ColN [46]. This suggest that no dramatic structural alterations occur because of polycationic resurfacing. Liu and co-workers in 2007 also demonstrated that engineered green fluorescent proteins with unusually high positive charges still emitted fluorescent light when exposed to UV lights [47]. In line with this, the binding of nanobodies [45] and the catalytic activity of enteropeptidase enzyme [48] were shown to be retained after replacing surface-exposed residues by genetic mutations. Therefore, with these engineering strategies in mind, certain resurfaced proteins remain functional similar to their wild-type one, implying that there are no changes in structural features. In terms of ColN stability determined by CD melting curve, the melting temperature of both proteins were relatively similar. Nevertheless, several precedent studies showed that resurfacing methods can improve the stability of the protein and prevent aggregation. GFP with extensive mutagenesis of solvent-exposed residues to charged residues were then created. These GFP variants containing either superpositive and supernegative net charges were resistance to aggregation and improved their thermostability [47]. Similarly, resurfaced single-chain antibody variable fragments (scFV) showing supercharge properties resisted heat denaturation and aggregation [49]. To enhance the thermal stability and endure the aggregation, ColN could undergo more extensive mutagenesis at solvent-accessible residues which can be achieved by constructing the charge variants of ColN. The increase in charges could result

in the thermal stability and the prevention of aggregation which could be further studied.

The main biological function of ColN is to kill bacterial cells by forming an ion channel in the inner membrane of susceptible bacteria [31]. Its mechanism of action requires all three domains to mediate bacterial cell death; i) R domain binds to outer membrane protein F and lipopolysaccharides (LPS) on the bacterial cell surface [50,51], ii) T domain interacts with receptors to trigger the translocation of P domain across bacterial membranes [52], and iii) P domain generates the pore causing ion leakage [53]. The spot test assay in this study revealed that the bactericidal activity of ColN⁺¹² was weaker than that of ColN^{WT}. The reduction of potency could be because the mutation at R domain may disrupt the interaction of this domain with outer membrane protein F and LPS on the surface of *E. coli*. The lack of interaction between R domain and its receptors could lead to the inefficient translocation of ColN⁺¹² to its target at the inner membrane of *E. coli*. On the other hand, the cytotoxicity towards human lung cancer cells significantly improved after polycationic resurfacing of R domain. The selective anticancer activity of both ColN against cancer cells were also presented. The improvement of these two properties corresponds with the former studies that demonstrated the influence of positively charged proteins on anticancer properties. Antimicrobial peptides (AMPs) with net positive charges have been proven to selectively kill cancer cells but not normal cells [54]. The exposed positively charged residues, lysine and arginine, on the surface of AMPs allow them to selectively interact with negatively charged cancer cell membrane [55]. This electrostatic interaction plays a vital role in the AMP cytotoxicity toward cancerous cells [28]. Unlike normal cell membranes, cancer cell membranes are comprised of more negatively charged molecules including phosphatidylserines, negative glycoproteins, as well as glycosaminoglycans [55]. For these reasons, ColN⁺¹² with polycationic features similar to AMPs could interact more strongly with cancer cells than with healthy cells. This results in the cancer-selective activity of ColN⁺¹². However, the pathway of how ColN⁺¹² causes a toxicity and induced apoptosis in cancer cells is still unclear. Even though ColN is classified as a pore-forming toxin, it did not mediate cytotoxic effect on lung cancer cells by membranolytic-based mechanisms. This mechanism kills cancer cells by forming a pore on cancer cell membrane resulting in membrane disruption. We have previously shown that ColN^{WT} alter the apoptosis-regulating proteins resulting in the elevation of apoptosis in ColN^{WT} treated lung cancer cells [17]. This mode of action could be due to the interaction of ColN^{WT} with receptors on the surface of lung cancer cells resulting in induction of apoptosis as discussed in Zandsalimi, F., et al., 2020 [56]. With structural similarity to ColN^{WT}, ColN⁺¹² with increasing positive surface charges would exert cytotoxic effects on cancer cells by the same mode of action. Cancer cells display the negative charge state of plasma membrane due to the incorporation of anionic molecules [54]. When increasing the surface positive charges of ColN, stronger electrostatic interactions between highly cationic ColN⁺¹² and cancer cell membranes could lead to the higher possibility of interaction with receptors of cancer cells which are involved in the apoptosis induction. Nevertheless, further studies could be performed to confirm the electrostatic interaction of ColN⁺¹² with cancer cells and the mechanism underlying cancer cell death caused by ColN⁺¹².

5. Conclusions

We have revealed that the mutagenesis of ColN by protein resurfacing approach can tailor the desired properties of ColN. It has shown that increase in the cationic properties of ColN by substitution of glutamic and aspartic acid with lysine can be achieved

without altering the structural features and thermal stability of ColN. Although the bactericidal activity of ColN mutant was reduced, the cytotoxicity of ColN mutant towards human lung cancer cells was significantly enhanced. Furthermore, the cancer-selective properties of ColN⁺¹² were observed. Therefore, protein resurfacing is a versatile tool which offers a development of desired features such as promotion of anticancer properties. The future direction for this research could be to investigate the mechanism of action of polycationic resurfaced ColN against various types of cancer cells. In addition, protein resurfacing approach could be used to modify other anticancer proteins to enhance their effectiveness.

Funding

WA was supported by grants from the Development and Promotion of Science Technology Talents (DPST) Research Grant, (grant number 024/2559) and the Faculty of Pharmaceutical Sciences, Chulalongkorn University (grant number Phar2560-RG02).

CRedit authorship contribution statement

Wanatchaporn Arunmanee: Conceptualization, Methodology, Formal analysis, Investigation, Data curation, Writing – original draft, Writing – review & editing, Visualization, Supervision, Project administration, Funding acquisition. **Methawee Duangkaew:** Formal analysis, Investigation, Data curation, Writing – original draft, Visualization. **Pornchanok Tawecheep:** Investigation. **Kanokpol Apicho:** Conceptualization, Methodology, Formal analysis, Investigation, Data curation, Writing – original draft, Visualization. **Panuwat Leardvorasap:** Investigation. **Jesada Pitchayakorn:** Investigation. **Chayada Intasuk:** Investigation. **Runglada Jiraratmetagon:** Investigation. **Armini Syamsidi:** Investigation. **Pithi Chanvorachote:** Resources. **Chatchai Chaotham:** Conceptualization, Methodology, Formal analysis, Data curation, Writing – original draft, Visualization, Supervision. **Natapol Pornputtpong:** Conceptualization, Methodology, Data curation, Writing – original draft, Writing – review & editing, Visualization, Supervision, Project administration, Funding acquisition.

Declaration of Competing Interest

The authors declare that they have no known competing financial interests or personal relationships that could have appeared to influence the work reported in this paper.

Acknowledgement

The authors would like to thank Dr. Helen Waller and Prof. Dr. Jeremy H. Lakey at Newcastle University, UK for providing ColN plasmids.

References

- [1] Yin L, Chen X, Vicini P, Rup B, Hickling TP. Therapeutic outcomes, assessments, risk factors and mitigation efforts of immunogenicity of therapeutic protein products. *Cell Immunol* 2015;295(2):118–26.
- [2] Mullard A. 2020 FDA drug approvals. *Nat Rev Drug Discov* 2021;20(2):85–90.
- [3] Samaranyake H, Wirth T, Schenkwein D, Rätty JK, Ylä-Herttuala S. Challenges in monoclonal antibody-based therapies. *Ann Med* 2009;41(5):322–31.
- [4] Dingermann T. Recombinant therapeutic proteins: production platforms and challenges. *Biotechnol J* 2008;3(1):90–7.
- [5] Scott AM, Wolchok JD, Old LJ. Antibody therapy of cancer. *Nat Rev Cancer* 2012;12(4):278–87.
- [6] Marcucci F, Bellone M, Rumio C, Corti A. Approaches to improve tumor accumulation and interactions between monoclonal antibodies and immune cells. *MAbs* 2013;5(1):34–46.

- [7] Wan L, Zeng L, Chen L, Huang Q, Li S, Lu Y, et al. Expression, purification, and refolding of a novel immunotoxin containing humanized single-chain fragment variable antibody against CTLA4 and the N-terminal fragment of human perforin. *Protein Expr Purif* 2006;48(2):307–13.
- [8] Avila AD, Mateo Acosta CD, Lage A. A carcinoembryonic antigen-directed immunotoxin built by linking a monoclonal antibody to a hemolytic toxin. *Int J Cancer* 1989;43(5):926–9.
- [9] Kheirandish MH, Jalilani HZ, Rahmani B, Nikukar H. Specific targeting of a pore-forming toxin (listeriolysin O) to LHRH-positive cancer cells using LHRH targeting peptide. *Toxicon* 2019;164:82–6.
- [10] Avila Ana D, Calderón Carlos F, Perez Rita M, Pons Carmen, Pereda Celia M, Ortiz Ana R. Construction of an immunotoxin by linking a monoclonal antibody against the human epidermal growth factor receptor and a hemolytic toxin. *Biol Res* 2007;40(2). <https://doi.org/10.4067/S0716-97602007000200008>.
- [11] Mutter NL, Soskine M, Huang G, Albuquerque IS, Bernardes GJL, Maglia G. Modular Pore-Forming Immunotoxins with Caged Cytotoxicity Tailored by Directed Evolution. *ACS Chem Biol* 2018;13(11):3153–60.
- [12] Okada M, Ortiz E, Corzo G, Possani LD, Silman I. Pore-forming spider venom peptides show cytotoxicity to hyperpolarized cancer cells expressing K⁺ channels: A lentiviral vector approach. *PLoS ONE* 2019;14(4):e0215391. <https://doi.org/10.1371/journal.pone.0215391>.
- [13] Tejuca M, Anderlugh G, Dalla Serra M. Sea anemone cytolytins as toxic components of immunotoxins. *Toxicon* 2009;54(8):1206–14.
- [14] Smarda J, Fialova M, Smarda J. Cytotoxic effects of colicins E1 and E3 on v-myb-transformed chicken monoblasts. *Folia Biol* 2001;47(1):11–3.
- [15] Chumchalová J, Smarda J. Human tumor cells are selectively inhibited by colicins. *Folia Microbiol* 2003;48(1):111–5.
- [16] Kaur S, Kaur S. Bacteriocins as potential anticancer agents. *Front Pharmacol* 2015;6.
- [17] Arunmanee W, Ecoy GAU, Khine HEE, Duangkaew M, Prompetchara E, Chanvorachote P, et al. Colicin N mediates apoptosis and suppresses integrin-modulated survival in human lung cancer cells. *Molecules* 2020;25(4):816. <https://doi.org/10.3390/molecules25040816>.
- [18] Fathizadeh H et al. Anticancer effect of enterocin A-colicin E1 fusion peptide on the gastric cancer cell. *Probiotics Antimicrob Proteins* 2021.
- [19] Lancaster LE, Wintermeyer W, Rodnina MV. Colicins and their potential in cancer treatment. *Blood Cells Mol Dis* 2007;38(1):15–8.
- [20] Kintzing JR, Filsinger Interrante MV, Cochran JR. Emerging strategies for developing next-generation protein therapeutics for cancer treatment. *Trends Pharmacol Sci* 2016;37(12):993–1008.
- [21] Chapman A, McNaughton B. Scratching the surface: resurfacing proteins to endow new properties and function. *Cell Chem Biol* 2016;23(5):543–53.
- [22] Der BS, Kluewe C, Miklos AE, Jacak R, Lyskov S, Gray JJ, et al. Alternative computational protocols for supercharging protein surfaces for reversible unfolding and retention of stability. *PLoS ONE* 2013;8(5):e64363. <https://doi.org/10.1371/journal.pone.0064363>.
- [23] Thompson DB, Cronican JJ, Liu DR. Engineering and identifying supercharged proteins for macromolecule delivery into mammalian cells. *Methods Enzymol* 2012;503:293–319.
- [24] Fuchs SM, Raines RT. Arginine Grafting to Endow Cell Permeability. *ACS Chem Biol* 2007;2(3):167–70.
- [25] Mitchell DJ et al. Polyarginine enters cells more efficiently than other polycationic homopolymers. *J Peptide Res* 2000;56(5):318–25.
- [26] Sundlass NK, Raines RT. Arginine residues are more effective than lysine residues in eliciting the cellular uptake of onconase. *Biochemistry* 2011;50(47):10293–9.
- [27] Felício MR, Silva ON, Gonçalves S, Santos NC, Franco OL. Peptides with dual antimicrobial and anticancer activities. *Front Chem* 2017;5. <https://doi.org/10.3389/fchem.2017.00005>.
- [28] Hoskin DW, Ramamoorthy A. Studies on anticancer activities of antimicrobial peptides. *Biochimica et Biophysica Acta (BBA) - Biomembranes* 2008;1778(2):357–75.
- [29] Bevers EM, Comfurius P, Zwaal RFA. Regulatory mechanisms in maintenance and modulation of transmembrane lipid asymmetry: pathophysiological implications. *Lupus* 1996;5(5):480–7.
- [30] Leaver-Fay A et al. ROSETTA3: an object-oriented software suite for the simulation and design of macromolecules. *Methods Enzymol* 2011;487:545–74.
- [31] Vetter IR, Parker MW, Tucker AD, Lakey JH, Pattus F, Tsemoglou D. Crystal structure of a colicin N fragment suggests a model for toxicity. *Structure* 1998;6(7):863–74.
- [32] Waterhouse A et al. SWISS-MODEL: homology modelling of protein structures and complexes. *Nucleic Acids Res* 2018;46(W1):W296–303.
- [33] Benkert P, Tosatto SCE, Schomburg D. QMEAN: a comprehensive scoring function for model quality assessment. *Proteins* 2008;71(1):261–77.
- [34] Schrodinger LLC. The AxPyMOL Molecular Graphics Plugin for Microsoft PowerPoint. Version 2015;1:8.
- [35] Schrodinger LLC. The PyMOL molecular graphics system. Version 2015;1:8.
- [36] Dolinsky TJ, Nielsen JE, McCammon JA, Baker NA. PDB2PQR: an automated pipeline for the setup of Poisson-Boltzmann electrostatics calculations. *Nucleic Acids Res* 2004;32(Web Server):W665–7.
- [37] Jurrus E et al. Improvements to the APBS biomolecular solvation software suite. *Protein Sci* 2018;27(1):112–28.

- [38] Hockett KL, Baltrus DA. Use of the soft-agar overlay technique to screen for bacterially produced inhibitory compounds. *J Visualized Experiments JOVE* 2017;119:55064.
- [39] Feoktistova M, Geserick P, Leverkus M. Crystal violet assay for determining viability of cultured cells. *Cold Spring Harb Protoc* 2016;2016(4). <https://doi.org/10.1101/pdb.prot087379>.
- [40] Herbst RS, Giaccone G, Schiller JH, Natale RB, Miller V, Manegold C, et al. Gefitinib in combination with paclitaxel and carboplatin in advanced non-small-cell lung cancer: a phase III trial-INTACT 2. *J Clin Oncol* 2004;22(5):785–94.
- [41] Koizumi T, Fukushima T, Gomi D, Kobayashi T, Sekiguchi N, Sakamoto A, et al. Alectinib-induced alopecia in a patient with anaplastic lymphoma kinase-positive non-small cell lung cancer. *Case Rep Oncol* 2016;9(1):212–5.
- [42] Chen P-H, Wang C-Y, Hsia C-W, Ho M-Y, Chen A, Tseng M-J, et al. Impact of taxol on dermal papilla cells—a proteomics and bioinformatics analysis. *J Proteomics* 2011;74(12):2760–73.
- [43] Shin SH, Cha HJ, Kim K, An I-S, Kim K-Y, Ku J-E, et al. Epigallocatechin-3-gallate inhibits paclitaxel-induced apoptosis through the alteration of microRNA expression in human dermal papilla cells. *Biomed Dermatol* 2018;2(1). <https://doi.org/10.1186/s41702-017-0016-1>.
- [44] Stanzl EG, Trantow BM, Vargas JR, Wender PA. Fifteen years of cell-penetrating, guanidinium-rich molecular transporters: basic science, research tools, and clinical applications. *Acc Chem Res* 2013;46(12):2944–54.
- [45] Bruce VJ, Lopez-Islas M, McNaughton BR. Resurfaced cell-penetrating nanobodies: a potentially general scaffold for intracellularly targeted protein discovery. *Protein Sci* 2016;25(6):1129–37.
- [46] Evans IJA, Labelle S, Cooper A, Bond LH, Lakey JH. The central domain of colicin N possesses the receptor recognition site but not the binding affinity of the whole toxin. *Biochemistry* 1996;35(48):15143–8.
- [47] Lawrence MS, Phillips KJ, Liu DR. Supercharging Proteins Can Impart Unusual Resilience. *J Am Chem Soc* 2007;129(33):10110–2.
- [48] Prasse AA, Zauner T, Büttner K, Hoffmann R, Zuchner T. Improvement of an antibody-enzyme coupling yield by enzyme surface supercharging. *BMC Biotech* 2014;14(1). <https://doi.org/10.1186/s12896-014-0088-6>.
- [49] Miklos A, Kluwe C, Der B, Pai S, Sircar A, Hughes R, et al. Structure-sibodies. *Chem Biol* 2012;19(4):449–55.
- [50] Johnson CL et al. The antibacterial toxin colicin N binds to the inner core of lipopolysaccharide and close to its translocator protein. *Mol Microbiol* 2014;92(3):440–52.
- [51] Jansen KB, Inns PG, Housden NG, Hopper JTS, Kaminska R, Lee S, et al. Bifurcated binding of the OmpF receptor underpins import of the bacteriocin colicin N into *Escherichia coli*. *J Biol Chem* 2020;295(27):9147–56.
- [52] Kleanthous C. Swimming against the tide: progress and challenges in our understanding of colicin translocation. *Nat Rev Microbiol* 2010;8(12):843–8.
- [53] Cascales E, Buchanan SK, Duché D, Kleanthous C, Lloubès R, Postle K, et al. Colicin biology. *Microbiol Mol Biol Rev* 2007;71(1):158–229.
- [54] Kunda NK. Antimicrobial peptides as novel therapeutics for non-small cell lung cancer. *Drug Discov Today* 2020;25(1):238–47.
- [55] Utsugi T et al. Elevated expression of phosphatidylserine in the outer membrane leaflet of human tumor cells and recognition by activated human blood monocytes. *Cancer Res* 1991;51(11):3062–6.
- [56] Zandsalimi F et al. Antimicrobial peptides: a promising strategy for lung cancer drug discovery? *Expert Opin Drug Discov* 2020;15(11):1343–54.